

# Design and Evaluation of the JSI-KneExo: Active, Passive, Pneumatic, Portable Knee Exoskeleton

Luka Mišković<sup>1,2</sup> Tilen Breclj<sup>1</sup> Miha Dežman<sup>3</sup> Tadej Petrič<sup>1,2</sup>

**Abstract**—This paper presents a portable stand-alone pneumatic knee exoskeleton that operates in both passive and active modes. The system can store and recover energy by means of compressed air in passive mode, leading to energy savings. In active mode, a small air pump inflates the pneumatic artificial muscle (PAM), which stores the compressed air, that can be then released into a pneumatic cylinder to generate torque. All electronic and pneumatic components are integrated into the system, and the exoskeleton weighs only 3.9 kg with a maximum torque of 20 Nm in the knee joint. Further, the system is modular, allowing wearability on one or both legs. The paper describes the mechatronic design, mathematical model and includes a validation study with an able-bodied subject performing sit-to-stand and squat-hold exercises. The results show that the exoskeleton can harvest energy while assisting the subject and reduce muscle activity, without compromising transparency. These results suggest that the presented exoskeleton could be a useful low-energy consumption device for individuals with low to moderate lower limb mobility impairments and improve endurance in both clinical and industrial settings.

**Index Terms**—Wearable Robotics, Prosthetics and Exoskeletons, Pneumatic Variable Stiffness, Energy Storage.

## I. INTRODUCTION

Limited mobility can have a detrimental impact on a person's quality of life. Mobility impairments can be caused by a variety of factors, including diseases, injuries, and aging. The human knee joint is essential for performing daily tasks and therefore its impairments can negatively affect them [1]. Alongside traditional assistive technologies such as passive orthoses and crutches, exoskeletons are wearable devices designed to augment and enhance a person's physical abilities and thus improve mobility [2]. Knee exoskeletons found in the literature are most often designed for the rehabilitation of patients or human performance augmentation of able-bodied individuals [3]. Commonly the actuators used are electromechanical [4]–[6] or pneumatic [7]–[9]. Electromechanical actuators are portable if powered by batteries, but to amplify torque from the electric motor, a transmission is required



Fig. 1. A person wearing the JSI-KneExo, a knee exoskeleton that can function in either active or passive mode. It is completely portable and has the ability to simultaneously assist the user and harvest energy.

which can introduce issues such as increased friction, reduced back-drivability, and decreased user comfort and safety [10]. Another difficulty with such types of actuators when used in portable exoskeletons is inertia and mechanical complexity that can quickly result in bulky exoskeletons compromising wearability when worn at distal limbs [11]. Variable stiffness actuators (VSAs) are a specialized type of electromechanical actuators that can generate positive net mechanical power and store elastic energy to provide assistance [12]. However, achieving transparency in these actuators without losing stored energy can be challenging and may require the use of brakes or clutches to detach the elastic element from the main lever.

Pneumatic actuators are another type of actuators that have been utilized in the knee and other exoskeletons and are attractive due to their inherent compliance and low mass. Examples in the literature include [7] weighing 0.8 kg (one leg only) and [8] weighing 4.5 kg (two legs), where both devices use pneumatic artificial muscles to generate torque. However, the need for an air tank presents a challenge to the portability of pneumatic exoskeletons. Only a few previous studies have successfully developed active portable pneumatic exoskeletons that integrate an onboard air compressor and a metal air tank. Examples of such studies include [13] weighing 9.12 kg, [14] weighing 9.95 kg, and [15] with a soft fabric actuator weighing 1.6 kg (one ankle only). In the last work, an air tank was not used, which resulted in lower actuation speed and limited force generation capability. The issue of limited

Manuscript received: Revised; Accepted

This work was supported by grants from the Slovenian Research Agency; PR-10489, and N2-0153.

<sup>1</sup>Luka Mišković, Tilen Breclj and Tadej Petrič are with the Department of Automatics, Biocybernetics and Robotics, Jožef Stefan Institute, Jamova cesta 39, 1000 Ljubljana, Slovenia, (Luka Mišković luka.miskovic@ijs.si)

<sup>2</sup>Luka Mišković and Tadej Petrič are with the Jožef Stefan International Postgraduate School, Jamova 39, 1000 Ljubljana, Slovenia,

<sup>3</sup>Miha Dežman is with the High Performance Humanoid Technologies (H2T), Institute for Anthropomatics and Robotics (IAR), Karlsruhe Institute of Technology (KIT), Adenauerring 2, 76131 Karlsruhe, Germany miha.dezman@kit.edu

Digital Object Identifier (DOI): see top of this page.

portability in pneumatic actuators was already addressed in our previous work, where in [16] we presented a method to modulate the stiffness of air springs by accumulating air from the atmosphere without an external air supply. This method was then applied and extended in the quasi-passive joint mechanism [17] to demonstrate how the accumulated air can be pumped into a pneumatic artificial muscle, providing a new type of variable stiffness.

**Contributions:** In this paper, the JSI-KneExo (Fig. 1) is introduced as a portable pneumatic knee exoskeleton capable of operating in both active and passive modes. The design is fairly slim and follows the leg contour without protrusion. Lightness is achieved by using a newly designed pneumatic actuator, which does not require heavy gears to generate high torque but instead uses a pneumatic cylinder and a soft PAM as an air tank, replacing heavy metal counterparts. Therefore the weight is only 3.9 kg making it one of the lightest portable active knee exoskeletons [3]. Another key contribution is the low energy consumption and energy harvesting capability while at the same time assisting the user. The important thing here is that the compressed air can be harvested and stored without compromising the transparency of the exoskeleton when needed, unlike the case with VSAs. Active mode is enabled by the onboard air pump charging the PAM, which then stores the compressed air and can release it in the pneumatic cylinder to create torque in the joint. In active mode, the exoskeleton can assist with tasks requiring net positive mechanical work in the knee joint, such as ascending stairs or

standing up. In passive mode, the exoskeleton acts as a damper, holding and supporting the knee. This means that when the knee flexes, the energy is stored and the generated torque tends to extend the knee back to its original position before flexion, thereby returning the energy to the wearer assisting against gravity. This way the exoskeleton saves energy and can assist the user, for example when squatting, descending stairs, or sitting down.

## II. THEORETICAL ANALYSIS

This section provides a mechatronic overview of the exoskeleton, its pneumatic design, and the mathematical model.

### A. Exoskeleton Overview

The JSI-KneExo (Fig. 2a) is a modular system made up of three major components: the left-leg exoskeleton with an actuator, the right-leg exoskeleton with an actuator, and the control unit. Depending on the application, one or both legs of the exoskeleton may be used simultaneously. The whole system weighs 3.9 kg (each leg of the exoskeleton 1.25kg and the control unit 1.4kg).

1) *The actuator unit:* The pneumatic actuator (Fig. 2b) comprises a pneumatic cylinder (DNSU-25-100-PPV-A, FESTO, Germany), which generates force when pressurized air enters its chamber. Because the cylinder is attached to the shank and thigh levers, the force in the cylinder causes torque in the joint. The cylinder has a maximum stroke of 100 mm and a bore diameter of 25 mm. The compressed air

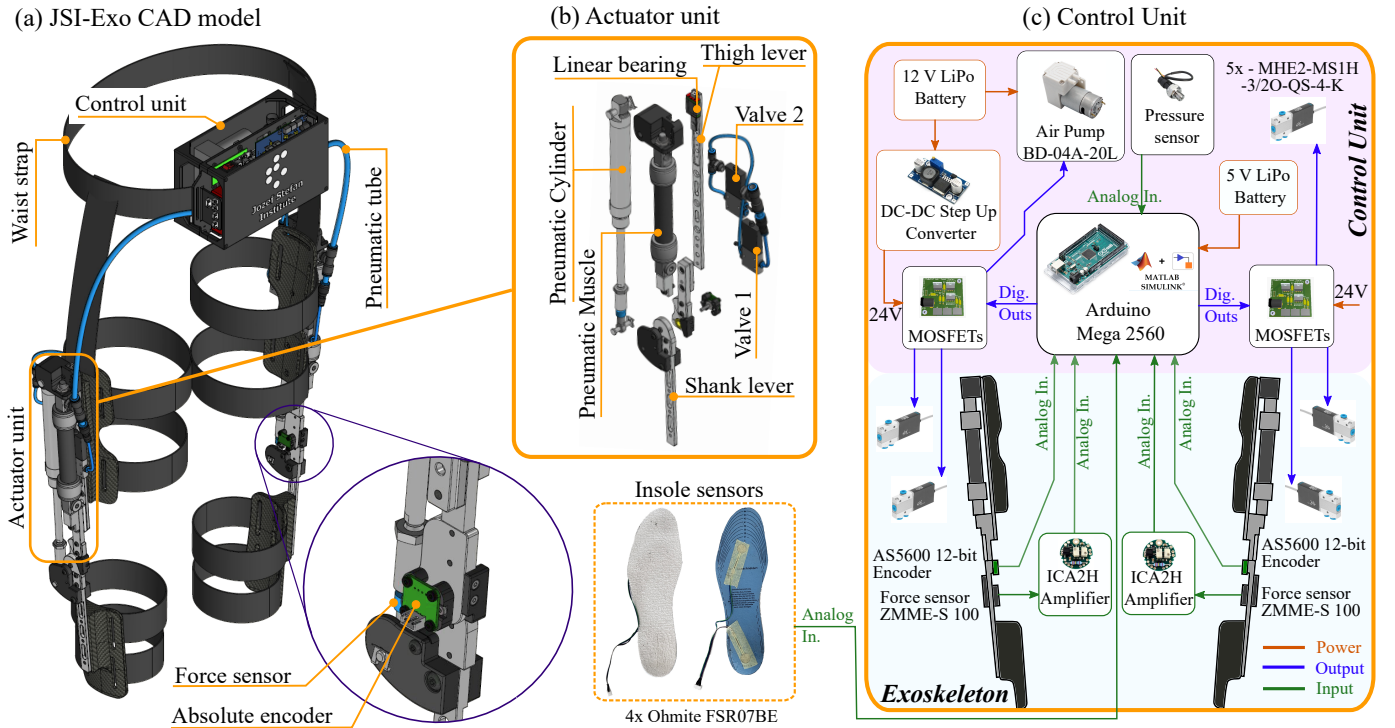


Fig. 2. The JSI-KneExo design. (a) The JSI-KneExo is made up of three modular parts: a control unit, a left-leg exoskeleton, and a right-leg exoskeleton. The waist strap is tightened and fastened with a buckle. The pneumatic tubing is routed from the control box to the PAM. (b) The actuator unit is made up of two air solenoid valves, a PAM, a pneumatic cylinder, a force sensor, an absolute encoder, a shank and thigh lever, and a linear bearing that allows the PAM to deflect linearly. (c) The pink background indicates all of the components in the control unit, whereas the light blue background indicates all of the components on the exoskeleton (legs) side. Optionally, insole sensors can be added when gait phase detection is required.

generated by the air pump is stored in the pneumatic muscle DMSP-20-100N-RM-RM (initial diameter 20mm, initial length 100mm), which when inflated shrinks its length and increases its diameter. The lower end of the PAM is fixed, while the upper-end slides on the linear bearing. Each actuator unit contains two solenoid air valves (MHE2-MS1H-3/2O-QS-4-K, FESTO, Germany) that allow state change, as detailed further in the paper. The absolute encoder AS5600 (ams-OSRAM AG, Austria) measures the joint angle, while the force in the cylinder is measured by the force sensor ZMME-S100 (Zhiminsensor, China).

2) *The control unit:* The control unit is shown in (Fig. 2c). Although pneumatic, the JSI-KneExo is fully portable as the compressed air is supplied by the air pump BD-04A-20L, BodenFlo, China, driven by a 12 V LiPo battery. If running continuously, the pump has an autonomy of  $\approx 3.4$  h. Two printed circuit boards each containing six MOSFET switches are used to change the position of the solenoid valves. An extra solenoid valve is included in the control unit box, the function of which is explained in the next section. A pressure sensor is integrated to continuously monitor the pressure in both PAMs. The voltage is converted to 24 V for the solenoid valves by the DC-DC Step Up. Optionally, insole sensors FSR07BE, Ohmite, USA, can be added for gait cycle recognition, which is not used in this paper. The main microcontroller is an Arduino Mega 2560.

### B. Portable pneumatic design

The portable pneumatic circuit is depicted in Fig. 3. All five solenoid valves are identical and monostable, allowing them to be easily switched from position '1' to position '2' with a switching frequency of  $\approx 2$  ms. The air pump produces compressed air, which charges the PAM and is monitored by a pressure sensor. The valve P depressurizes the tube once it has

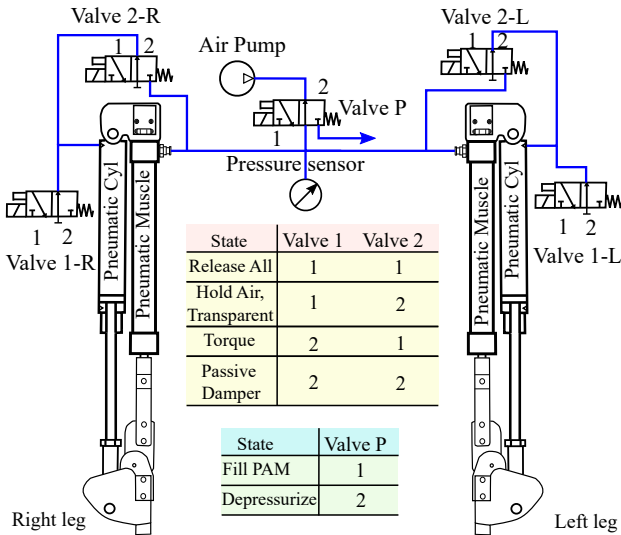


Fig. 3. Pneumatic circuit of the JSI-KneExo. Different valve positions achieve different exoskeleton states.

been filled with air; otherwise, when the air pump is restarted, the reverse pressure will hold the pump back when it needs the most power. Both sides (left and right) have symmetrical

pneumatic connections. Different valve combinations achieve various states. For example, in "Release all" both valves 1 and 2 are set to '1', implying that the air is released and the atmospheric pressure fills the cylinder and the PAM. The second state, "Air Hold, Transparent," implies that the air pump fills the PAM to the desired pressure set in the control algorithm, but valve 1 has a clutch function, which means that if in position '1,' the pneumatic cylinder will not generate force as the chamber is connected to the atmosphere and air cannot be compressed. After the actuator has been in the transparent state, by switching valve 2 to position '1' compressed air enters the cylinder chamber and generates the force in the cylinder, and the torque in the joint. It is important that valve 1 is switched back to position '2', as otherwise, the air would be discharged. This state is called the "Torque" state or active mode. The last state is the "Passive Damper" or passive mode, in which both valves are set to position '2'. Torque is generated as the air inside the cylinder is compressed by knee flexion, and it behaves like a non-linear progressive compression spring that resists rotation. Furthermore, in this state, compressed air can be brought back to the PAM by flexing the joint and switching valve 2 back to position 1 so that air flows back into the PAM.

### C. Mathematical model

1) *Air pump:* The air pump has the function of charging the PAM with compressed air up to the desired pressure. Commercially available air pumps are rated for no-load air flow when the pressure is 0 bar. Therefore, it is problematic to calculate the time required to fill the PAM as the pressure increases. A less precise and merely approximate way would be to estimate the average flow to calculate the time required to fill the PAM. Another approach is to experimentally identify the relationship between pressure and time. Therefore, two

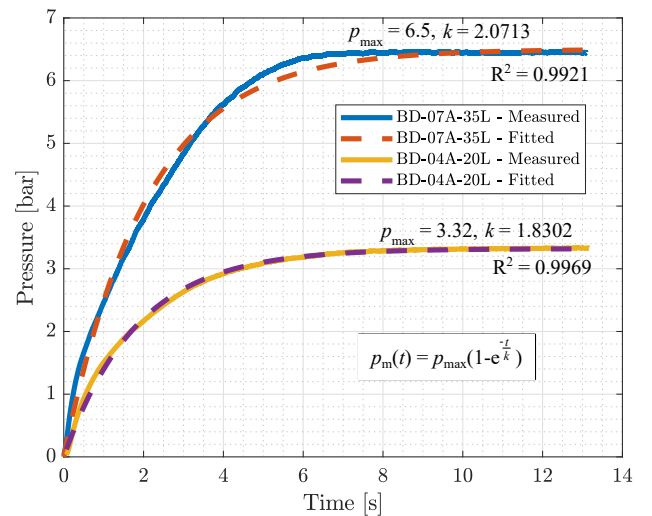


Fig. 4. Filling compressed air into the PAM with two different pumps, the larger BD-07A-35L and the smaller BD-04A-20L. The equation fitted through measured data has the form:  $p_m(t) = p_{\max}(1 - e^{-t/k})$ . For the larger pump:  $p_{\max} = 6.5$  bar,  $k = 2.0713$ , and  $R^2 = 0.9921$ . For the smaller pump:  $p_{\max} = 3.32$  bar,  $k = 1.8302$  and  $R^2 = 0.9969$ .

commercially available air pumps were experimentally identi-

fied and compared; BD-04A-20L, with a maximum pressure of 3.5 bar and a flow rate of 20 L/min at 0 bar, and the air piston pump BD-07A-35L with a maximum pressure of 6.5 bar and a flow rate of 35 L/min at 0 bar. Fig. 4 shows the measured pressure over time when filling the pneumatic muscle DMSP-20-100N-RM-RM with air for both pumps. The measured data were fitted with the following exponential function:

$$p_m(t) = p_{\max}(1 - e^{-\frac{t}{k}}), \quad (1)$$

where  $p_m(t)$  is the actual pressure at time  $t$ ,  $p_{\max}$  is the maximum nominal pressure for the pump, and  $k$  is the pump constant identified for both pumps. The coefficient of determination is  $R^2 = 0.9921$  for BD-07A-35L, while for BD-04A-20L it is  $R^2 = 0.9969$ .

The time required to reach  $p_{\max}$  in the PAM for the chosen pump may now be determined with Eq. (1).

2) *Pneumatic Artificial Muscle (PAM)*: When the air gets compressed inside the PAM, its length  $L_m$  and volume  $V_m$  change. The analytical dependency  $V_m(L_m)$  is known and adopted from [18]. However, with a known PAM pressure  $p_m$  its length  $L_m$  can only be approximated from the FESTO datasheet for the exact PAM or other existing PAM models [18], [19]. As FESTO only provides graphs without an analytical model, it cannot be used in further calculations for the JSI-KneExo. Other models are either for static cases or are specific to the PAM used and their accuracy cannot be determined with certainty for the PAM selected in this paper. Still, the dependency between the pressure  $p_m$ , length  $L_m$ , and the volume  $V_m$  is needed to compute the torque in the actuator. Therefore, the model was determined experimentally by compressing air into the PAM and measuring the contraction, denoted as  $\varepsilon$ . The PAM force was zero in the experiment since the linear bearing allows unrestrained contraction.

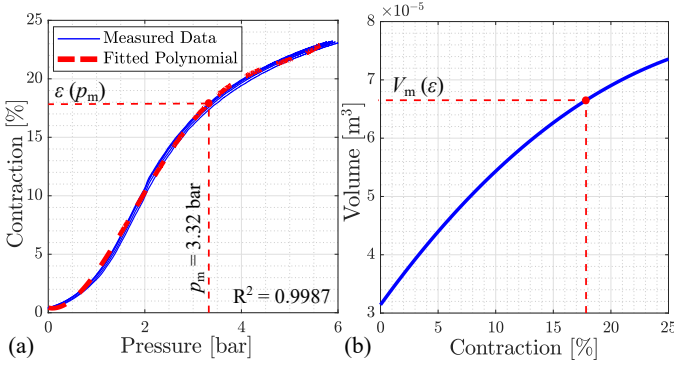


Fig. 5. Model-identification of the PAM DMSP-20-100N-RM-RM. In (a) PAM contraction versus pressure. In (b) PAM volume versus contraction. For a given pump pressure, it is possible to determine the PAM volume.

The experimental identification is shown in Fig. 5, where (a) shows the measured contraction  $\varepsilon$  as a function of PAM pressure  $p_m$ , and (b) shows the analytical model linking PAM volume  $V_m$  and contraction  $\varepsilon$ , given in Eq. 3, for different contractions where the maximum contraction for the chosen PAM is equal to 25%. The measured data were fitted with a fourth-degree polynomial, formulated as

$$\varepsilon(p_m) = c_1 p_m^4 + c_2 p_m^3 + c_3 p_m^2 + c_4 p_m + c_5, \quad (2)$$

where the coefficients are  $c_1 = 0.1022$ ,  $c_2 = -1.3370$ ,  $c_3 = 5.1426$ ,  $c_4 = -0.8131$ ,  $c_5 = 0.4189$ , with the coefficient of determination  $R^2 = 0.9987$ .

Using the identified relation  $\varepsilon(p_m)$ , the contraction  $\varepsilon$  and hence the length  $L_m$  of the PAM for each pressure  $p_m$  can be obtained as  $L_m = L_0 - \varepsilon$ , where  $L_0$  is the initial PAM length. This also allows the determination of the PAM volume,  $V_m$ , for each length  $L_m$ , which was previously unknown. The PAM volume can be calculated according to [18] as follows

$$V_m = \frac{L_m L_f^2 - L_m^3}{4\pi n_{tu}^2}, \quad (3)$$

where  $n_{tu}$  is the number of thread turns, and  $L_f$  is the thread length calculated according to [19]. Now this relationship can be used to calculate the torque in the exoskeleton which is explained in the next subsection.

3) *Actuator Pressure, Force, and Torque*: the mathematical model of the actuator is given for one side exoskeleton leg and is further derived according to Fig. 6, where the transition from (a)→(b) implies standing up and reversely sitting down, meaning that in (a)→(b) the pressure is released from the PAM and shared with the pneumatic cylinder, while in (b)→(a) the pressure is returned to the PAM. The initial angle in (a) is  $\theta = 107^\circ$ , as this is the angle at which the piston rod comes to the end of the cylinder, for contraction  $\varepsilon(p_m = 3.32 \text{ bar})$ , which is identified as a maximum pressure for the selected air pump BD-04A-20L. At the point where the angle  $\theta$  starts

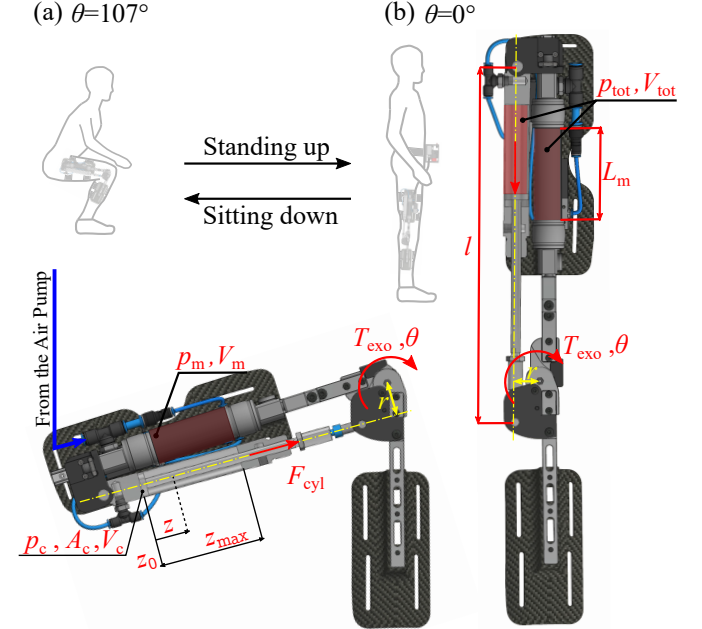


Fig. 6. Model of the exoskeleton. In (a) the exoskeleton is flexed to the angle  $\theta = 107^\circ$  which is the angle at which  $z = z_0$  for contraction  $\varepsilon(p_m = 3.32 \text{ bar})$ . In (b) the exoskeleton is at angle  $\theta = 0^\circ$  meaning that the wearer is standing.

decreasing, the air valve connecting the cylinder and the PAM is switched to position '1' as explained earlier. This results in two volumes merging, and the common volume is defined as:

$$V_{\text{tot}} = V_c + V_m, \quad (4)$$

where  $V_c$  is the volume of the cylinder with the volume of the pneumatic tube added and is equal to

$$V_c = A_c z + A_{tc} l_{tc}, \quad z \in [z_0, z_{max}], \quad (5)$$

where  $A_{tc}$  is the cross-sectional surface area of the pneumatic tube and  $l_{tc}$  is its length from the cylinder to the PAM. The current position of the piston  $z$  is expressed as

$$z = z_{max} \frac{l - l_{min}}{l_{max} - l_{min}}, \quad (6)$$

where  $l$  is the cylinder length (Fig. 6b), which was previously derived in our article [17], and  $l_{min}$  is the length when the piston touches the end of the cylinder ( $z = z_0$ ). The maximum actuator length  $l_{max}$  is the length for  $z = z_{max}$ .

The PAM volume was given in Eq. 3, but now the volume of the pneumatic tube ( $A_{tm} l_{tm}$ ) is added for the actuator as follows

$$V_m = \frac{L_m L_f^2 - L_m^3}{4\pi n_{tu}^2} + A_{tm} l_{tm}. \quad (7)$$

Once the total volume is known, and isothermal expansion is assumed, the air pressure  $p_{tot}$  expanding from the initial pressure  $p_{tot}^{init}$  and the initial volume  $V_{tot}^{init}$  to the current volume  $V_{tot}$  can be computed as

$$p_{tot} = p_{tot}^{init} \frac{V_{tot}^{init}}{V_{tot}}, \quad (8)$$

As volume  $V_{tot}$  gradually increases, pressure  $p_{tot}$  decreases, which means that as the angle  $\theta$  approaches  $0^\circ$  (knee fully extended),  $L_m$  also decreases, consequently affecting the cylinder length  $l$ , the current position of the piston  $z$ , and finally the volume of the cylinder  $V_c$ . Therefore, the PAM length must be updated for each new pressure during the transition according to the model identified in Eq. 2.

Once the current pressure is known during the transition, the cylinder force  $F_{cyl}$  can be expressed as the pressure  $p_{tot}$  acting on the piston surface area  $A_c$ , as follows

$$F_{cyl} = p_{tot} A_c. \quad (9)$$

Finally, with the known cylinder force  $F_{cyl}$ , the exoskeleton torque  $T_{exo}$  can be computed as follows

$$T_{exo} = F_{cyl} r, \quad (10)$$

where the lever arm  $r$  (see Fig. 6) was mathematically modeled in our previous article [17]. The computed values of different physical parameters for the joint rotation from  $\theta = 107^\circ$  to  $\theta = 0^\circ$  are shown in Fig. 7.

In the case when the angle  $\theta$  is changed from  $\theta = 0^\circ$  to  $\theta = 107^\circ$  (sitting down), the process is reversed if the "Torque" state is still active. Therefore, by rotating the joint back to  $\theta = 107^\circ$  the air is compressed back into the PAM while generating the same torque.

However, when the "Passive Damper" state is activated (see Fig. 3) at the angle of  $\theta = 0^\circ$  and the joint is rotated back to  $\theta = 107^\circ$ , the air is compressed only in the cylinder's volume, thus the pressure and torque reach much higher values than in the active mode. Still, the air can be returned back into the PAM by setting valve 2 in position '1' once the air has been compressed in the cylinder (person sitting).

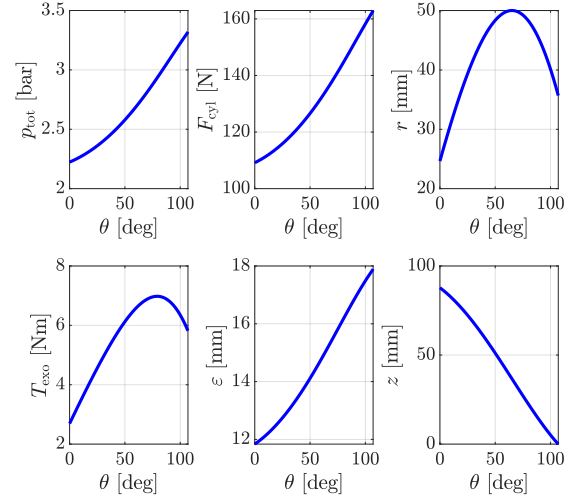


Fig. 7. Theoretical profiles of different physical parameters for the joint rotation from  $\theta = 107^\circ$  to  $\theta = 0^\circ$ .

4) *Limitations of the mathematical model:* The mathematical model within the scope of this paper does not account for dynamical stretching of the PAM that occurs when the cylinder's force exceeds the PAM's static force for a given pressure. Positively stretching the PAM requires much more force, [20], compared to the force in the pneumatic cylinder. Another case in which the PAM dynamical stretching occurs is when the angle exceeds  $\theta = 107^\circ$ . Therefore, the behavior was not theoretically modeled for angles beyond, although rotation is possible up to  $\theta = 135^\circ$ . The experimental results will identify the exoskeleton's dynamics as a whole.

### III. THE JSI-KNEEXO EVALUATION

The following section presents the results of a pilot study conducted with an able-bodied subject (27 years old, weighing 90 kg, and standing at a height of 1.93 m). The study aimed to validate the main mechatronic contributions of the JSI-KneExo. The exoskeleton was controlled in Simulink Real-Time™, while the pressure, angle, and force data were collected and analyzed offline in Matlab. The experimental setup is depicted in Fig. 8. To determine whether the exoskeleton affects the subject, a multi-channel surface EMG system was used (Trigno wireless, Delsys, USA) recording at 2148.15 Hz. The EMG electrodes were placed according to the SENIAM guidelines [21]. The activity of two muscles involved in sitting transfers, the Vastus Medialis (V. Med.) and the Gluteus Maximum (Glut. M.), was recorded on each leg. Before the experiments, the maximum voluntary contraction (MVC) was recorded for each muscle, respectively. Joint kinematics was measured with 16 cameras from the Optitrack system (NaturalPoint, USA) recording at 120 Hz. A total of 37 reflective markers were attached to the subject according to the Motive Optical motion capture software to reconstruct the human skeleton. The screen in front of the subject provided visual feedback and displayed the subjects' initial and current positions during the experiment to ensure that the subjects' positioning was repeatable in all repetitions.

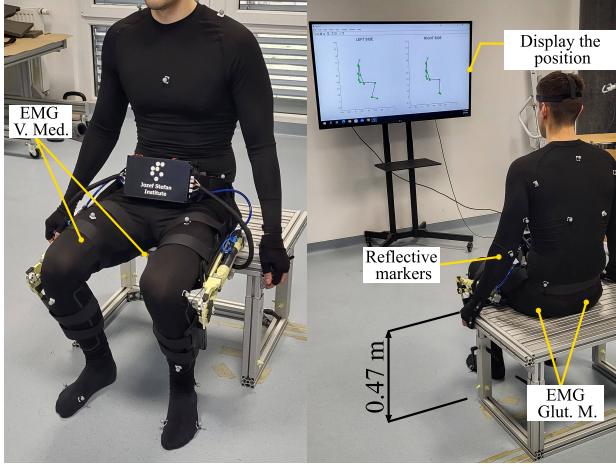


Fig. 8. Experimental setup. The screen displays the initial and current position of the human skeleton in the left and right sagittal planes. EMG electrodes and reflective markers were placed as indicated.

### A. Experiments

The subject was instructed to perform two different tasks, the first of which was performing ten transitions from sitting to standing and from standing to sitting in unassisted (transparent) and assisted conditions. The second experiment involved holding a squat for 30 s, unassisted and then assisted, with each test being repeated five times with a 5-minute pause in between to avoid fatigue.

1) *Experiment1: Sit-Stand*: The main objective of this experiment is to demonstrate that the exoskeleton can return the compressed air to the PAM (recover energy) while relieving the leg muscles, and also to evaluate the exoskeleton operation, highlighting the transparency achieved after every sit-down. When standing up, the exoskeleton assisted the subject in active mode, and when sitting down, the exoskeleton assisted the subject in passive mode. In the unassisted trial, the state was set to "Release All", allowing the actuator to rotate freely.

**Strategy and Control**: The controller for assisted condition consists of a state machine and the states are triggered based on threshold values from a pressure sensor and two encoders, where the angular velocity of the knee is calculated as a numerical differentiation of the knee angle. The exoskeleton torque was calculated offline by multiplying the measured cylinder force and the lever arm length, which was calculated from the knee angle and mathematical model.

Figure 9 shows a graph of the average exoskeleton (right leg) torque and its standard deviation over ten repetitions with respect to the transition identified from the knee angle, where 100% corresponds to sitting and 0% to standing. Figure 10 shows the pressure change in both PAMs connected together since the pressure sensor is directly connected to them (see Fig. 3). The intervals when the pump was switched on and off are indicated as well as the amount of air that was returned. In both figures, the exoskeleton states are indicated by numbers. The experiment is divided into the seven following parts.

**Initial Sitting**: The experiment started in ① by equalizing the actuator with the atmospheric pressure. The air pump started in ② and gradually filled the PAM with compressed

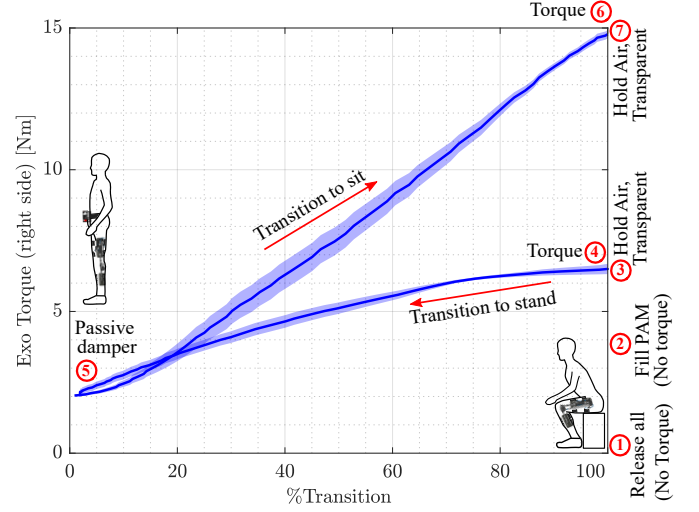


Fig. 9. Experiment1: Torque in the right leg exoskeleton with respect to the transition, where 100% corresponds to the sitting and 0% to the standing position. The different states are indicated by the numbers in circles.

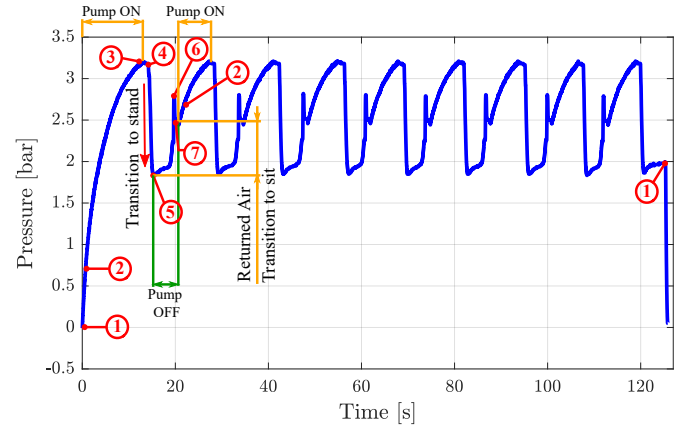


Fig. 10. Experiment1: Measurement of the pressure sensor over time. The different modes are indicated by numbers. Intervals, when the pump is on and off, are indicated, as well as returned air.

air to the desired pressure, which was set to 3.2 bar. In ③ the air pump was switched off as the PAM was charged with compressed air but had not yet been released into the cylinder and therefore the exoskeleton was still transparent.

**Standing Up**: When the sensors detected that the subject had started standing up in ④, the compressed air was released into the pneumatic cylinder, providing an active torque of  $\approx 6.7$  Nm which gradually decreased as the pressure dropped until ⑤ (fully standing), at which point the pressure was equal to  $\approx 1.84$  bar and the torque  $\approx 2$  Nm.

**Sitting Down**: Upon sensor detection of the standing position, the mode was changed to "Passive damper". Therefore, from ⑤ to ⑥, when the subject transitioned to the sitting position, the air was compressed exclusively in the pneumatic cylinder, reaching a maximum torque of  $\approx 14.88$  Nm.

**Air Return**: By detecting that the person was fully seated, in ⑥, and by setting valve 2 to position '1', the compressed air from the cylinder had flown back into the PAM, where the pressure in the PAM was then equal to  $\approx 2.5$  bar. Thus

the pressure was restored from  $\approx 1.84$  bar to  $\approx 2.5$  bar as the subject went from standing to sitting.

**Transparent Sitting:** In ⑦ the "Hold Air, Transparent" state was activated to allow unobstructed seating by releasing the remaining compressed air from the cylinder.

**Next Repetition:** In the next repetition, the air pump only had to compensate for the air loss because the joint was not fully rotated to its minimum position (see Fig. 6a). Thus, the air pump was restarted in ②, which allowed the PAM to be refilled up to 3.2 bar.

**End:** Finally, all the compressed air from the actuator was released in ① and the experiment was completed.

**Experiment 1 - Muscle Effort:** Fig. 11 shows the average muscle activity of ten repetitions during the transitions between sitting and standing positions for both unassisted (ExoOff) and assisted (ExoOn). The mean envelope of the raw EMG signals was extracted to analyze the effects on muscle effort. The signals were first filtered with a 4<sup>th</sup> order bandpass Butterworth filter with cut-off frequencies from 20-400 Hz. The signals were then rectified and low pass filtered (5 Hz, 4<sup>th</sup> order Butterworth filter). The EMG amplitude was then normalized to the subject's MVC, segmented, and averaged with respect to %Sitting and %Standing, identified from the knee angle.

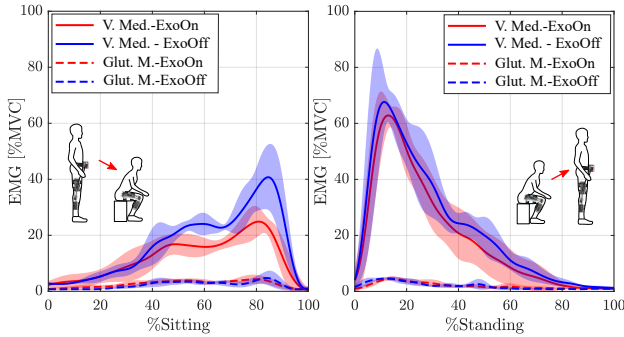


Fig. 11. Experiment1: Sit-Stand. EMG recordings of the vastus medialis and gluteus maximus during sitting and standing transfers under both assisted and unassisted conditions.

#### EMG reduction with simultaneous energy recovery:

Interestingly, when the compressed air was returned to the exoskeleton reservoir, not only was energy and pumping time saved, but the exoskeleton also reduced muscular effort. It is notable that V. Med. activity decreased considerably when sitting down with exoskeleton assistance, compared to when the exoskeleton was transparent. No major changes in Glut. M. were observed between two conditions, and activity was quite low when normalized to MVC. When standing up, there is a slight decrease in V. Med. activity when the exoskeleton assisted compared to the unassisted condition. This was to be expected because the assisting torque for standing up was lower than for sitting down.

2) *Experiment 2: Holding the squat for 30 seconds:* The main objective of this experiment is to evaluate whether the generated torque can be consistent when holding the squat position due to possible air leakage. In this experiment, the exoskeleton was running in the "Torque" state, but the subject's initial position was standing upright as both the

pneumatic cylinder and the PAM were filled with compressed air at 3.2 bar. The subject was instructed to squat and hold the position for 30 seconds, five times unassisted and five times assisted.

The results of the second experiment are shown in Fig. 12. The results indicate that Glut. M. activity was greater when holding a squat position compared to the first experiment. There is an observable decrease in muscle activity for both measured muscles. Most importantly, the torque versus time plot reveals that there is only a slight change in torque over 30 seconds, from  $\approx 16.71$  Nm to  $\approx 15.9$  Nm, while the knee angle remained almost the same. These findings provide additional support for the concept of the actuator applied in the JSI-KneExo.

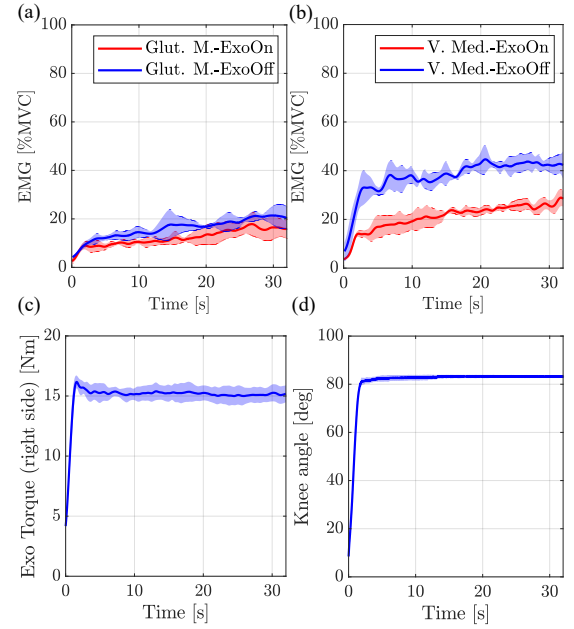


Fig. 12. Experiment2: Squat hold; (a) EMG recordings of the gluteus maximus, (b) EMG recordings of the vastus medialis, (c) Torque in the right leg exoskeleton, (d) Right knee angle.

## IV. DISCUSSION

Table I details the relevant parameters of the JSI-KneExo. The exoskeleton is portable and lightweight due to the new pneumatic actuation configuration. The total weight including

TABLE I  
TECHNICAL SPECIFICATIONS OF THE JSI-KNEEXO

PARAMETER	VALUE
Total weight <sup>1</sup>	3.9 kg
One Exo Leg weight	1.25 kg
Control unit weight	1.4 kg
Max. Pressure	8 bar
Max. Torque <sup>2</sup>	20 Nm
Range of Motion	0-135 deg
Battery life <sup>3</sup>	$\approx 3.4$ h

<sup>1</sup> Actuator weight breakdown: air cylinder (238g), valves ( $2 \times 60$ g), PAM (200g)

<sup>2</sup> Obtained at max. pressure of 8 bar and max. lever arm ( $r = 50$ mm).

<sup>3</sup> Assuming continuous operation without energy harvesting.

the battery is 3.9 kg, of which the control unit weighs 1.4

kg, and the left and right legs 1.25 kg each. The maximum pressure handled by the pneumatic components is 8 bar. The maximum torque is determined using the maximum pressure in the cylinder. The system uses electrical energy only to power the air valves and the air pump with a battery life of  $\approx 3.4$ h assuming continuous operation without energy harvesting. The novel pneumatic circuit design includes five solenoid valves that enable different modes for the exoskeleton, allowing for either discharging air, transparent movement, passive mode, or active mode.

Despite its advantages, the JSI-KneExo has some limitations. First, the pneumatic pump produces a noise of approximately 60 dB, which may be uncomfortable in public spaces. Second, the frequency of actuation is constrained by the air pump's capacity and the target pressure. Using a larger air pump would increase the charging speed of the PAM, but would also add weight and noise. Additionally, the effects of the exoskeleton on the wearer's kinematics were not investigated in this study and remain to be studied in further research.

## V. CONCLUSION

In conclusion, the key innovation of the JSI-KneExo is simultaneous energy harvesting and human augmentation without compromising transparency. Other innovations are portable pneumatic actuation, lightness achieved with the novel actuator and using PAM as an air tank, low energy consumption, and pneumatic circuit design that provides different operation modes, of which transparency is crucial when no assistance is needed. The pneumatic actuation mechanism used in the JSI-KneExo has the potential for application in other robots, such as legged or jumping robots, expanding its range of potential uses beyond just exoskeletons. Future work will focus on investigating the efficacy of JSI-KneExo in assisting with walking and analyzing the effects on a larger sample of subjects to conclude whether the developed prototype could be useful in industrial settings or for people with low to moderately reduced mobility to assist with activities of daily living.

## REFERENCES

- [1] A. H. Alnahdi, J. A. Zeni, and L. Snyder-Mackler, "Muscle Impairments in Patients With Knee Osteoarthritis," *Sports Health*, vol. 4, no. 4, pp. 284–292, 2012.
- [2] G. S. Sawicki, O. N. Beck, I. Kang, and A. J. Young, "The exoskeleton expansion: Improving walking and running economy," *Journal of NeuroEngineering and Rehabilitation*, vol. 17, no. 1, pp. 1–9, 2020.
- [3] B. Chen, B. Zi, Z. Wang, L. Qin, and W. H. Liao, "Knee exoskeletons for gait rehabilitation and human performance augmentation: A state-of-the-art," *Mechanism and Machine Theory*, vol. 134, pp. 499–511, 2019. [Online]. Available: <https://doi.org/10.1016/j.mechmachtheory.2019.01.016>
- [4] M. Cestari, D. Sanz-Merodio, J. C. Arevalo, and E. Garcia, "An adjustable compliant joint for lower-limb exoskeletons," *IEEE/ASME Transactions on Mechatronics*, vol. 20, no. 2, pp. 889–898, 2015.
- [5] M. K. Shepherd and E. J. Rouse, "Design and Validation of a Torque-Controllable Knee Exoskeleton for Sit-to-Stand Assistance," *IEEE/ASME Transactions on Mechatronics*, vol. 22, no. 4, pp. 1695–1704, 2017.
- [6] K. Schmidt, J. E. Duarte, M. Grimmer, A. Sancho-Puchades, H. Wei, C. S. Easthope, and R. Riener, "The myosuit: Bi-articular anti-gravity exosuit that reduces hip extensor activity in sitting transfers," *Frontiers in NeuroRobotics*, vol. 11, no. OCT, pp. 1–16, 2017.
- [7] D. Maeda, K. Tominaga, T. Oku, H. T. Pham, S. Saeki, M. Uemura, H. Hirai, and F. Miyazaki, "Muscle synergy analysis of human adaptation to a variable-stiffness exoskeleton: Human walk with a knee exoskeleton with pneumatic artificial muscles," *IEEE-RAS International Conference on Humanoid Robots*, no. 1, pp. 638–644, 2012.
- [8] K. Knaepen, P. Beyl, S. Duerinckx, F. Hagman, D. Lefeber, and R. Meeusen, "Human-robot interaction: Kinematics and muscle activity inside a powered compliant knee exoskeleton," *IEEE Transactions on Neural Systems and Rehabilitation Engineering*, vol. 22, no. 6, pp. 1128–1137, 2014.
- [9] P. Malcolm, S. Galle, W. Derave, and D. de Clercq, "Bi-articular knee-ankle-foot exoskeleton produces higher metabolic cost reduction than weight-matched mono-articular exoskeleton," *Frontiers in Neuroscience*, vol. 12, no. MAR, pp. 1–14, 2018.
- [10] B. van Nijhuijs, L. A. van der Heide, J. W. Jansen, B. L. Gysen, D. J. van der Pijl, and E. A. Lomonova, "Overview of actuated arm support systems and their applications," *Actuators*, vol. 2, no. 4, pp. 86–110, 2013.
- [11] J. Kim, G. Lee, R. Heimgartner, D. A. Revi, N. Karavas, D. Nathanson, I. Galiana, A. Eckert-Erdheim, P. Murphy, D. Perry, N. Menard, D. K. Choe, P. Malcolm, and C. J. Walsh, "Reducing the metabolic rate of walking and running with a versatile, portable exosuit," *Science*, vol. 365, no. 6454, pp. 668–672, 2019.
- [12] J. Sun, Z. Guo, Y. Zhang, X. Xiao, and J. Tan, "A Novel Design of Serial Variable Stiffness Actuator Based on an Archimedean Spiral Relocation Mechanism," *IEEE/ASME Transactions on Mechatronics*, vol. 23, no. 5, pp. 2121–2131, 2018.
- [13] M. Wehner, B. Quinlivan, P. M. Aubin, E. Martinez-Villalpando, M. Baumann, L. Stirling, K. Holt, R. Wood, and C. Walsh, "A lightweight soft exosuit for gait assistance," *Proceedings - IEEE International Conference on Robotics and Automation*, pp. 3362–3369, 2013.
- [14] U. Heo, S. J. Kim, and J. Kim, "Backdrivable and Fully-Portable Pneumatic Back Support Exoskeleton for Lifting Assistance," *IEEE Robotics and Automation Letters*, vol. 5, no. 2, pp. 2047–2053, 2020.
- [15] C. M. Thalman, J. Hsu, L. Snyder, and P. Polygerinos, "Design of a soft ankle-foot orthosis exosuit for foot drop assistance," *Proceedings - IEEE International Conference on Robotics and Automation*, vol. 2019-May, pp. 8436–8442, 2019.
- [16] L. Miskovic, M. Dezman, and T. Petric, "Pneumatic Quasi-Passive Variable Stiffness Mechanism for Energy Storage Applications," *IEEE Robotics and Automation Letters*, vol. 7, no. 2, pp. 1705–1712, 2022.
- [17] —, "Pneumatic Exoskeleton Joint with a Self-Supporting Air Tank and Stiffness Modulation: Design, Modeling, and Experimental Evaluation," *TechRxiv. Preprint.*, 2023.
- [18] M. Martens and I. Boblan, "Modeling the static force of a Festo pneumatic muscle actuator: A new approach and a comparison to existing models," *Actuators*, vol. 6, no. 4, pp. 1–11, 2017.
- [19] C. P. Chou and B. Hannaford, "Measurement and modeling of McKibben pneumatic artificial muscles," *IEEE Transactions on Robotics and Automation*, vol. 12, no. 1, pp. 90–102, 1996.
- [20] Festo, "Fluidic Muscle DMSP," *MAS, Operation instructions, FESTO, Esslingen, . . .*, 2007. [Online]. Available: <https://www.festo.com/media/pim/554/D15000100140554.PDF>
- [21] H. J. Hermens, B. Freriks, C. Disselhorst-Klug, and G. Rau, "Development of recommendations for SEMG sensors and sensor placement procedures," *J. Electromyogr. Kinesiol.*, vol. 10, no. 5, p. 361–374, 2000.